DETERMINATION OF MATERIAL PARAMETERS OF A TEXTILE REINFORCED COMPOSITE USING AN INVERSE METHOD

J. Blom, H. Cuypers, P. Van Itterbeeck and J. Wastiels

VUB in Brussels -Faculty of Engineering , Department of Mechanics of Materials and Constructions, Pleinlaan 2, 1050 Brussels, Belgium,
johan.blom@vub.ac.be

ABSTRACT

A great diversity of different cement based fibre reinforced concrete (FRC) materials can be found today either in practical use or under development in research laboratories. The main goal of using fibres in a cement based matrix is to improve the ductility. A FRC is called a high performance material when the use of fibres leads to tensile strain hardening. This can only be obtained by using a fibre volume fraction which is exceeding the critical volume fraction. If so the fibres can ensure strength and stiffness at applied loads far exceeding the range in which matrix multiple cracking occurs. Textile reinforced cementitious composites with glass fibres as reinforcement exhibit relatively high strength and ductility and thus provide and interesting new material for construction purposes. The textile reinforced concrete (TRC) under study in this paper is essentially composed of two brittle materials. In this case a random distributed glass fibre textile is used in combination with an inorganic phosphate cement matrix. The material itself is characterised by a linear behaviour in compression and a non linear tensile behaviour. However, in order to design and optimize constructions it is not only necessary to develop effective analysis and design guidelines but also a method to obtain the necessary model parameters. In this paper an inverse method is presented to derive the model parameters which are normally obtained from a tensile test. The model parameters can be defined as the ultimate matrix stress and the efficiency of the fibres and matrix. The proposed inversed method uses the experimental force- deflection curves obtained from a four point bending test to derive the model parameters.

1. INTRODUCTION

Textile reinforced cementitious composites with glass fibre reinforcement are new composite materials which can be tailored to the needs and specifications of the constructive elements. By using a fibre volume fraction which is exceeding the critical fibre volume fraction, the fibres can ensure strength and stiffness at applied loads far exceeding the range in which matrix multiple cracking occurs. The TRC composites are interesting new high performance materials. Freeform architecture and lightweight construction elements (e.g. sandwich panels with TRC faces [1] and hypar shells [2]) only represent a small part of the construction types where the advantages of this material could be exploited. If however we want to design and optimize a construction with a new material the development of a material model is necessary. Over the years much effort has been directed into the modelling of the non linear tensile behaviour. The behaviour in tension and compression of the above mentioned material is well documented in literature. The Aveston Cooper and Kelly (ACK) theory is one of the earliest developed models [3, 4]. In compression, this material exhibits a linear elastic behaviour up to failure. Since the use of fibre reinforcement in the form of textiles

allows the introduction of a high fibre volume fraction, a distinct strain hardening behaviour can be obtained in tension [5]. In an initial step based on the ACK theory, the bending behaviour of slender TRC beams can be analytically described [6, 7]. For each cross section the equilibrium of forces and moments can be calculated. Subsequent integration of the bending stiffness for each differential beam element with a certain height and a unit width, over the total length, will result in a computed force displacement diagram. The main goal of this paper is to propose a model which enables the user to derive the model parameters which enable the user to derive the parameters which are normally obtained from a tensile test, from data obtained from a bending test. The model parameters are the efficiency of the matrix (η_{matrix}), the efficiency of the fibres (η_{fibre}) and the ultimate matrix stress (σ_{mu}). The material parameters can be defined as the stiffness in the uncracked stage, the composite multiple cracking stress and the stiffness of the composite in cracked stage. The proposed inverse method uses the experimental force deflection curves obtained from a four point bending test. To determine the influence of model parameters on the computed bending behaviour a parametric study was preformed.

2. MODEL

2.1 TRC in tension and compression

In this paper the stress – strain behaviour in tension will be modelled using the ACK theory. In this model, the mechanical behaviour of unidirectional (UD) continuous fibre reinforced brittle matrix composites is described. Basic assumptions of the ACK theory are:

- The fibres can only cope with loads along their longitudinal axis, they provide no bending stiffness.
- There is a weak bond between fibre and matrix
- Once the matrix and fibres are debonding a pure frictional shear replaces the existing adhesion shear bond.
- The frictional shear is assumed to be constant
- Poisson effects of the fibre and matrix are neglected.
- The load distribution in the cross section perpendicular to longitudinal axis is assumed to be uniform.

2.2. ACK theory.

According to the ACK theory, three distinct stages can be detected in the stress-strain curve of a unidirectional reinforced brittle matrix composite. In the first stage the material behaves linear elastic. The composite stiffness in stage I (Ec1) can be derived from the law of mixtures see equation (1). In this first stage a prefect “elastic” bond between matrix and fibres is assumed. The failure strain of the matrix is lower than the failures strain of the fibres. At the ultimate matrix strain the composite will crack. If the fibre volume fraction is higher than the critical fibre volume fraction, the fibres will be able to sustain the additional loading. According to the ACK theory this stage is called the “multiple cracking” stage. In the third stage ” post cracking” the matrix is completely crack. The fibre will carry the load in this final stage, until failure. Figure 1 illustrates a theoretical stress-strain curve with these three distinct stages (used in the ACK theory): linear elastic stage (I), multiple cracking stage (II) and post cracking stage (III).

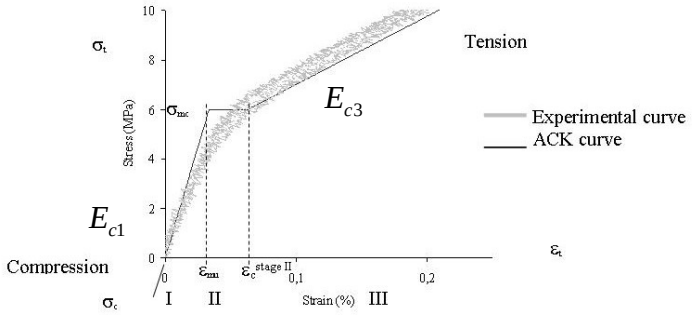

Fig.1: experimental and theoretical stress-strain curve, according to the ACK theory [3]

In the linear elastic stage (stage I), according to the ACK theory, the stiffness of the composite E_{c1} is function of the fibre volume fraction V_f, the volume fraction of the matrix V_m, the stiffness of the fibres E_f and the stiffness of the matrix E_m. The matrix-fibre interface bond is assumed to be elastic and the composite stiffness E_{c1} can be determined by the law of mixtures:

$$E_{c1} = E_f V_f + E_m V_m \quad (1)$$

The ACK theory is modified, due to imperfect matrix-fibre adhesion, warping or misalignment of the unidirectional fibres, inclusion of air voids, etc. the fibre volume fraction has to be lowered with a fibre efficiency factor η_f . Also the stiffness of the matrix has to be reduced with a matrix efficiency factor η_m . The modified law of mixtures can be written as followed.

$$E_{c1} = E_f V_f^* + E_m V^*_m \quad (2)$$

The effective fibre volume fraction can be calculated by using the following equation :

$$V_f^* = V_f \cdot \eta_f \quad (3)$$

Taking the efficiency of the matrix in account results in the following equation:

$$V_f^* = V_m \cdot \eta_m \quad (4)$$

When the first crack is introduced the ultimate strain of matrix (ε_{mu}) and composite multiple cracking strain (ε_{mc}) are equal. The composite multiple cracking stress (σ_{mc}) can be determined by the following equation (5) with (σ_{mu}) defined as the ultimate matrix stress.

$$\sigma_{mc} = \frac{\sigma_{mu} E_{c1}}{E_m} \quad (5)$$

When the first crack appears and reaches a fibre, debonding of the matrix-fibre interface occurs and further matrix-fibre interaction occurs through friction. The frictional interface stress (τ_o) is assumed to be constant along the debonding interface.
The debonding length δ_0 can be calculated from the equilibrium of the forces along the crack. In case of circular fibres with a radius (r) the following expression (6) can be used to derive the debonding length.

$$\delta_0 = \frac{\sigma_{mu} . r . V_m}{2 . \tau_0 . V_f} \quad (6)$$

Increasing the load will lead to multi cracking, if the fibre volume fraction is increasing the critical volume fraction. According to the ACK theory at a certain unique composite stress σ_{mc}, multiple parallel cracks are introduced in the matrix. Cracks are introduced

until saturation is reached. The distance between neighbouring cracks are situated between δ_o and $2\delta_o$, with an average of 1,337 δ_o. After multiple cracking, the strain of the composite $\varepsilon_c^{stageII}$ can be calculated as follows(7) .(from integration of the strain field between two cracks with distance 1,337)

$$\varepsilon_c^{stageII} = (1+0.66\alpha)\varepsilon_{mu} \quad (7)$$

$$\text{with} \quad \alpha = \frac{E_m V_m}{E_f V_f^*} \quad (8)$$

Once full multiple cracking has occurred, only the fibres further dedicate to the stiffness in stage III (post-cracking stage). The stiffness of the composite E_{c3} in this stage is thus:

$$E_{c3} = E_f V_f^* \quad (9)$$

2.3 TRC beam element in bending

Since the behaviour of TRC in tension shows three stages, three expressions are needed to define the equilibrium of forces and moments if a specimen is loaded in bending. By expressing the equilibrium of forces and moments, the position of the neutral axis (which will be further written as a) and the maximum occurring tensile strain (ε_t) in the section can be calculated for each cross section along the beam. Subsequent integration of the bending stiffness for each differential beam element with height h and a unit width, over the total length, will lead to a force displacement diagram. For each cross section one of the following sets of equilibrium equations can be used depending on the value of the maximum tensile stress. As long as the composite behaves linear elastic along the whole beam section the following expressions can be used, with M_e defined as external moment:

$$a = h/2 \quad (10)$$

$$M_e = \frac{2}{3} a^2 E_{c1} \varepsilon_t \quad (11)$$

Once the composite maximum tensile strain is situated in the multiple cracking stage the equilibrium equations can be based on the internal strains and stresses in figure 2 a.

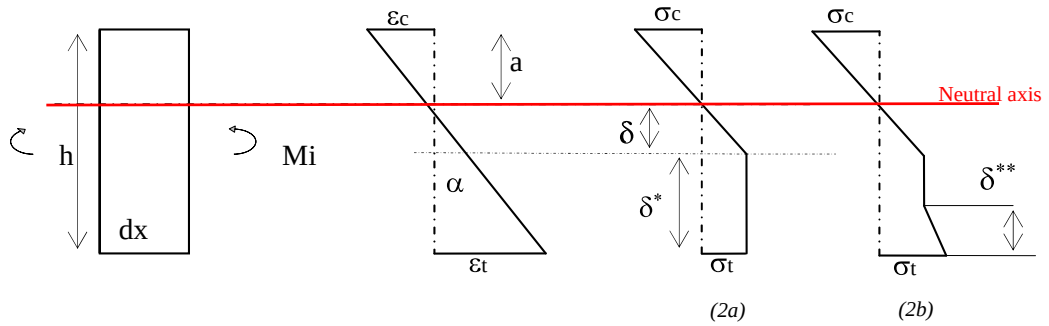

Fig. (2) distribution of stress and strain over cross section
(2a) distribution of stress strain over cross section in the multiple cracking stage
(2b) distribution of stress strain over cross section in the post cracking stage

By expressing the equilibrium of forces (12) and moments (13), the position of the neutral axis and the maximum occurring tensile strain (ε_t) in the section can be calculated for each cross section along the beam.

$$E_{c1}\varepsilon_t \frac{a^2}{2(h-a)} = \delta \frac{\sigma_{mc}}{2} + \delta^* \sigma_{mc} \quad \text{with } \delta = \frac{\varepsilon_{mu}}{\varepsilon_t}(h-a) \quad \text{and } \delta^* = h - a - \delta \tag{12}$$

$$E_{c1}\varepsilon_t \frac{a^3}{3(h-a)} + \delta^2 \frac{\sigma_{mc}}{3} + \sigma_{mc}\delta^* (\delta + \frac{\delta^*}{2}) = M_e \tag{13}$$

Finally the composite maximum tensile strain will be situated in the post-cracking stage. By expressing the equilibrium of forces (14) and moments (15), the position of the neutral axis and the maximum occurring tensile strain (ε_t) in the section can be calculated for each cross section along the beam.

$$E_{c1}\varepsilon_t \frac{a^2}{2(h-a)} = \delta \frac{\sigma_{mc}}{2} + \delta^* \sigma_{mc} + (\varepsilon_t - \varepsilon_c{}^{stageII}) E_f V_f{}^* \frac{\delta^{**}}{2} \quad \text{with } \delta^{**} = h - a - \frac{\varepsilon_c{}^{stageII}}{\varepsilon_{mu}}\delta \tag{14}$$

$$E_{c1}\varepsilon_t \frac{a^3}{3(h-a)} + \delta^2 \frac{\sigma_{mc}}{3} + \sigma_{mc}\delta^* (\delta + \frac{\delta^*}{2}) + (h - a - \frac{\delta^{**}}{3}) \frac{\delta^{**}}{2} (\varepsilon_t - \varepsilon_c^{stageII}) E_f V_f^* = M_e \tag{15}$$

Once the equilibriums of all sections are established, the deflection in any section can be determined by double integration of M_e /$EI_{section}$ along the length of the beam. $EI_{section}$ is the bending stiffness as calculated for each section of the beam.

2.4 Sensitivity analysis:

The sensitivity analysis showed that certain model parameters (e.g. the ultimate matrix stress, fibre efficiency and matrix stiffness) have a considerable influence on the modelled bending behaviour. Figure (3 a) is representing the tensile stress strain curve obtained from the analytical solution based on the ACK theory. The parameters used in this calculation are listed in the table below.

Em	18	GPa	matrix stiffness
Ef	72	GPa	fibre stiffness
ε max	1.5	%	composite ultimate strain
η_{fibre}	0.27		Efficiency of the fibres
η_{matrix}	1		Efficiency of the matrix
l	200	mm	Length
B	50	mm	Width
H	7.56	mm	Thickness
nfl	10		Number of layers
σ mu	2 up to 12 (step 2)	MPa	matrix ultimate stress

Table1: input parameters used in the parametric study

The bending model simulated a 4 point bending test with a span of 200 mm between the supports and a distance of 100 mm between the applied forces. For each tensile stress – strain curve the resulting force deflection curve is plotted (3 b). Increasing the ultimate matrix stress (σ_{mu}) will not only enlarge the linear elastic stage in bending stage, but will also accentuate the non linear behaviour.

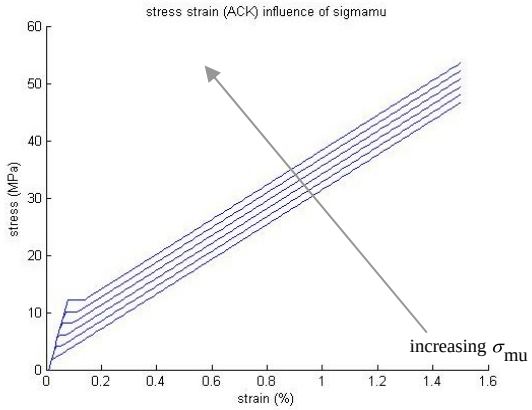

Figure 3 a: computed tensile stress – strain curve, showing the influence of σ_{mu}

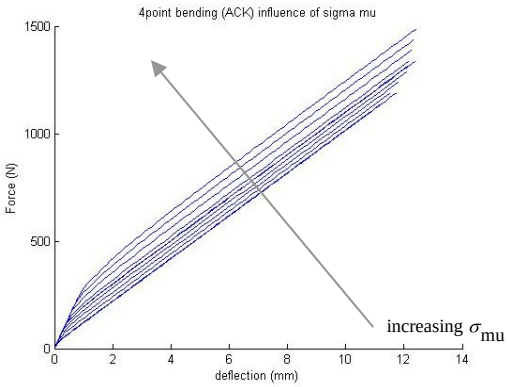

Figure 3 b: computed force displacement curves in 4 point bending

The stiffness in the third stage is increasing by the influence of the efficiency of the fibre reinforcement (η_f). This is clearly shown in figure (4 a) which is representing the tensile stress strain curve obtained from the analytical solution based on the ACK theory. The force displacement curve shows the same trend as the tensile stress strain curve. Changing the fibre efficiency from 0.05 up to 0.3 with a step of 0.05 mainly affect the last part of the force displacement, this is shown in figure (4 b). The fibre efficiency was limited to 0.3 according value obtained for 2 D random fibres (6).

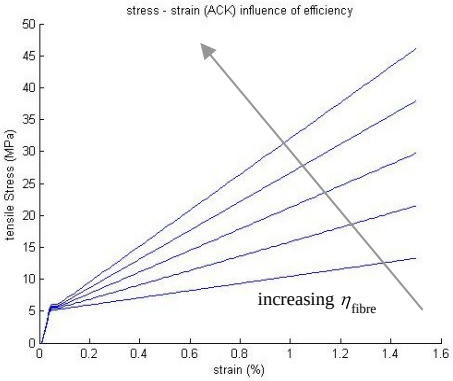

Fig:ure 4 a: computed tensile stress – strain curve, showing the influence of fibre efficiency

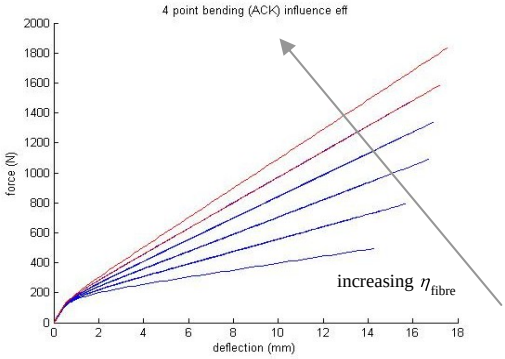

Figure 4 b: computed force displacement curves in 4 point bending

The effect of changing the matrix stiffness between 5 up to 25 GPa with a step of 5 GPa is plotted in the stress – strain curve figure (5 a). When observing the curves it is clear that the effect of changing the matrix stiffness is small. When observing the tensile stress curves it is clear that the effect of changing the matrix stiffness only affects the first zone.

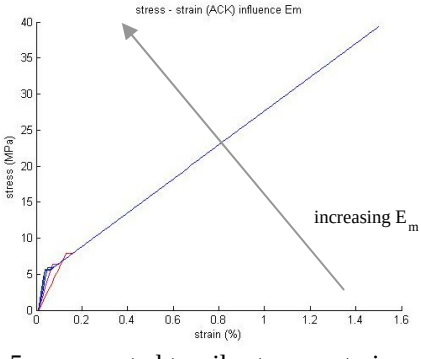

Figure 5 a: computed tensile stress – strain curve, showing the influence of matrix stiffness

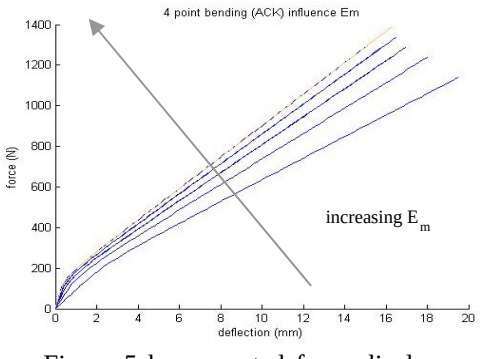

Figure 5 b: computed force displacement curves in 4 point bending

Figure 5 b shows the influence of the matrix stiffness on the deflection in 4 point bending when the maximum tensile strain is kept constant (1.5%). It's clear that the matrix stiffness influences the complete behaviour of the composite. When increasing the matrix stiffness, the effect on the nonlinear behaviour on the force deflection curves is increasing.

3. INVERSE METHOD

The inverse method developed within the scope of this paper allows the user to determine a set of model parameters ($\eta_{matrix}, \eta_{fibre}, \sigma_{mu}$) with a certain degree of accuracy. The set of model parameters contains the efficiency of the matrix (η_{matrix}), the efficiency of the fibres (η_{fibre}) and the ultimate matrix stress (σ_{mu}). At first the experimental force deflection curve obtained from a four point bending test will be loaded in the program. The inverse method will use the bending model based on the ACK theory. The program will generate for each set of three parameters ($\eta_{matrix}, \eta_{fibre}, \sigma_{mu}$) an analytical force displacement curve. The process is repeated until the difference between the experimental and analytical force displacement curve is minimized, using the coefficient of determination (R^2) [10].

4. EXPERIMENTS

The experimental part was preformed to obtain force deflection curves from 4 point bending test which were used in the inverse method as input data. To verify the proposed inverse method, tensile tests were also preformed.

4.1 Specimen preparation

The specimens used in this paper were glass fibre- reinforced cementitious laminates. The cementitious matrix used for all the specimens is an Inorganic Phosphate Cement (IPC)[11]. IPC has been developed at the "Vrije Universiteit Brussel" and shows a neutral pH after hardening. Therefore, the fibres are hardly attacked by the concrete matrix with time. The material properties of hardened IPC are similar to those of other cement-based materials. Although the strength in compression is rather high, the tensile strength is low. The tensile strength of an IPC specimen is about one tenth of the compressive strength. One standard IPC mixture is chosen in this work, without use of any fillers or retards or accelerating components. All IPC laminates are made by hand lay-up and cured in ambient conditions for 24 hours. Post-curing is performed at 60°C for 24 hours. Like most cementitious mixtures, the strength of IPC increases with time. This effect can however be accelerated by the post-curing at 60°C. During the curing and post-curing process, both sides of the laminate are covered with plastic to prevent early evaporation of water. The E-glass fibre reinforcements used in the specimens was chopped glass fibre mats ("2D-random") with a fibre density of 300g/m² (Owens Corning M705-300). The dimension of the plate is 50cmx50cm. The plates were produced with an average matrix consumption of 1200 g/m² for each layer. The plates were cut with a water cooled diamond saw. About four cut strip specimens had a width of 25mm and six others had a width of 50mm. The specimens with a width of 25mm are used for tensile testing and the specimens with a width of 50mm were tested in bending.

4.2 Bending test

For each laminate, several specimens were loaded in a 4 point bending test. Two supports were placed with a span of 200 mm, the crosshead was equipped with horizontal bars were two cylinder were mounted with a distance of 100 mm. By moving the cross head at a constant speed the cylinders will transfer a force to the specimen. The force on the cross head and the displacement in the centre of the laminate were measured. The testing machine was displacement controlled; the loading rate was set to 1 mm/min.

4.3 Tensile testing

The tensile test was carried out to obtain the ACK-model parameters for all tested laminates. The stress strain curve data was generated using a tensile testing machine with a capacity of 100 kN. The rate of cross head displacement was set at 1 mm/min. The strain was measured with an extensometer. The resulting stress-strain curves for a 6 layers random reinforced TRC are plotted and discussed here.

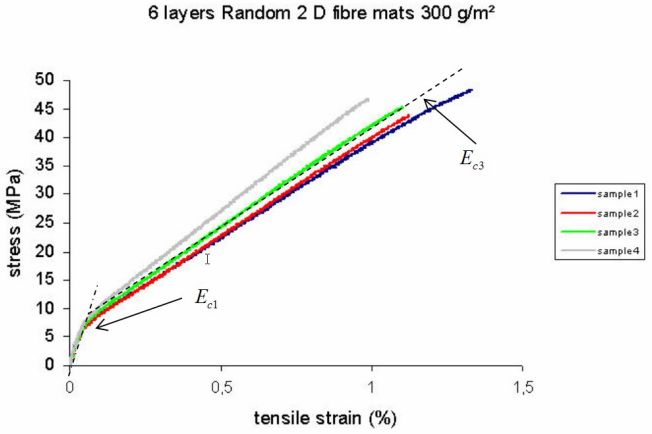

Figure 8: shows the stress-strain curves obtained on the specimens from plate 2 (with 6 layers of fibres)

The stiffness in the first (Ec1) and the third stage (Ec3) can be obtained from the experimental data by determination of the slope of the curves. The values of Ec1 and Ec3 are listed below in table 2. The model values obtained from the experimental data are printed cursive.

Plate number	Number of layers	Thickness (mm)	V_f (%)	E_{c1} (GPa) experimental	E_{c3} (GPa) experimental	η_{matrix}	η_{fibre}	σ_{mu}(GPa)
1	4	2.9	16.24	11.675	3.061	*0.57*	*0.26*	*7.91*
2	6	4.2	16.83	14.585	3.266	*0.76*	*0.27*	*7.50*
3	8	5.1	18.60	11.810	3.099	*0.59*	*0.23*	*6.29*
4	10	7.6	15.62	10.955	2.757	*0.54*	*0.25*	*5.32*
5	12	8.4	16.91	15.015	3.479	*0.77*	*0.29*	*8.31*
avg			16.84	12.808	3.13	0.65	0.26	7.07
stdev			1.11	1.853	0.27	0.11	0.02	1.23

Table 2: overview of the experimental data

5. COMPARISON BETWEEN MODEL PREDICTIONS AND EXPERIMENTS

To illustrate the inverse method the tensile stress curves are generated with the material parameters ($\eta_{matrix}, \eta_{fibre}, \sigma_{mu}$) obtained from the inverse method which uses the experimental force deflection curves. In this case the force deflection curves (fig. 9) of a six layer random specimen are used in the inverse method. .

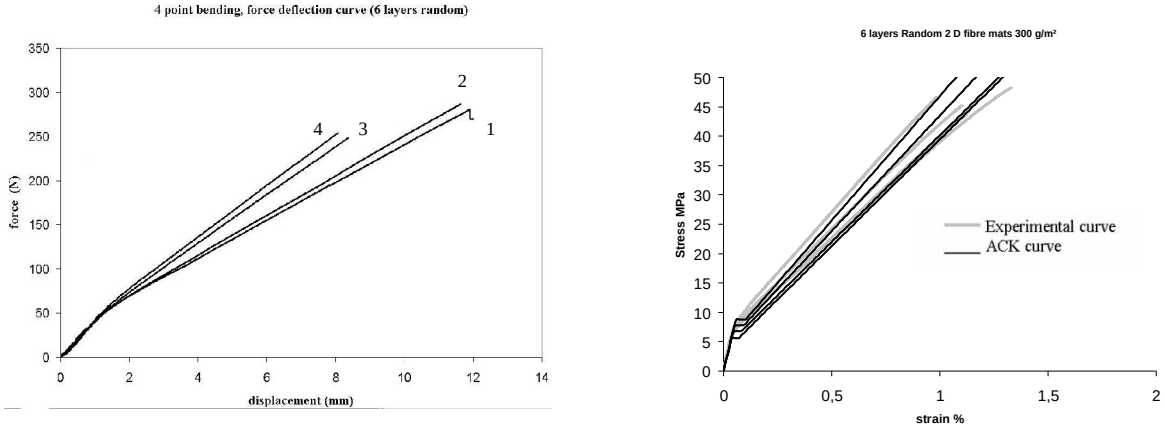

Figure 9: experimental obtained force displacement curves of a 6 layers random specimen and the stress – strain curves computed with the inverse method.

For each force displacement curve as set of parameters ($\eta_{matrix}, \eta_{fibre}, \sigma_{mu}$) is derived as shown in table below.

F- δ curve	s_{mu} (MPa)	η_{matrix}	η_{fibre}	Ec1 (GPa)	Ec3 (GPa)	R^2
1	5.06	0.75	0.300	14.863	3.636	0.99
2	6.19	0.75	0.325	15.166	3.938	0.99
3	8.23	0.75	0.325	15.166	3.938	0.99
4	8.27	0.75	0.350	15.469	4.241	0.99
avg	6.94	0.75	0.325	15.166	3.938	0.99
stdev	1.58	0.00	0.020	0.247	0.246	

Table 3: values obtained from the inverse method (6 layers random)

The inverse method was used to obtain the parameter of the other specimens. For each set of specimens with the same amount of layers the average of parameters were plotted in the table below (4). The values in the thicker rectangle are derived by the inverse method.

n_{fl}	η_{matrix}	η_{fibre}	σ_{mu} MPa	η_{matrix}	$\Delta\eta_m$	η_{fibre}	$\Delta\eta_f$	σ_{mu} MPa	$\Delta\sigma_{mu}$ MPa
4	0.57	0.26	7.91	0.60	0.03	0.250	0.010	8.75	0.84
6	0.76	0.27	7.50	0.75	0.01	0.325	0.055	6.94	0.56
8	0,60	0.23	6.29	0.60	0.01	0.225	0.005	7.15	0.86
10	0.54	0.25	5.32	0.55	0.01	0.250	0.000	6.30	0.98
12	0.77	0.29	8.31	0.80	0.03	0.300	0.010	8.50	0.19
a_{vg}	0.65	0.26	7.07	0.66		0.270		7.47	
stdev	0.11	0.02	1.23	0.11		0.040		1.10	

Table 4: average values obtained from the inverse method

When comparing the experimental model parameters and the values obtained from the inverse method it is clear that the influence of the thickness can be neglected. The values of the model parameters ($\eta_{matrix}, \eta_{fibre}, \sigma_{mu}$) derived from the inverse method are close to the experimental. In table 4 the difference between experimental and analytical model parameters is listed ($\Delta\eta_{matrix}, \Delta\eta_{fibre}, \Delta\sigma_{mu}$).

6. CONCLUSIONS

The inverse method developed within the scope of this paper allows the user to determine a set of model parameters ($\eta_{matrix}, \eta_{fibre}, \sigma_{mu}$). Comparing the experimental and analytical values of the model parameters showed that the difference is smaller than the standard deviation which means that the proposed inverse model is capable to compute the parameters with accuracy. When comparing the experimental model parameters and the values obtained from the inverse method it is clear that the influence of the thickness on the model parameters can be neglected.

REFERENCES

(1) Cuypers H., Analysis and Design of Sandwich panels with Brittle matrix composite faces for building applications, Phd. Thesis, VUB 2002

(2) E. De Bolster , H. Cuypers, K. Watzeels, G. Mosselmans, M. Alshaaer ,Numerical analysis of a modular system consisting of hyperbolic paraboloids, made of a cementitious composite, Department of mechanics and constructions, Vrije Universiteit Brussel, Belgium

(3) Aveston, J.; Cooper, G.A.; Kelly, A.: *Single and multiple fracture. The properties of fibre composites* Proceedings Conf. National Physical Laboratories, IPC Science & Technology Press Ltd., *London*, UK, Nov. 1971, p15.

(4) Aveston J., Mercer R.A. and Sillwood J.M., "The mechanism of fibre reinforcement of cement and concrete" ,SI No 90/11/98, January 1975, DMA 228, February 1976

(5) Naaman A. E., Toughness, ductility, surface energy and deflection-hardening FRC composites, Proceedings of the JCI international Workshop on Ductile Fiber Reinforced Cementitious Composites (DFRCC) - Application and Evaluation (DFRCC-02), Takayama, Japan, October, 2002, pp 33-57.

(6) Cox H;L;, The elasticity and strength of paper and other fibrous material, Britisch Journal of Applied Physics, Vol.3,1952,p.72-79

(7) J. Blom , H. Cuypers P,. Van Itterbeeck, J. Wastiels, Modelling the behaviour of Textile Reinforced Cementitious composites under bending, Prague, Fibre Concrete 4th International Conference, p.205-210, 2007

(8) Maalej M., Li V.C.," Flexural/Tensile-Strength Ratio in Engineered Cementitious Composites", Journal of Materials in Civil Engineering Vol 6.no4, November 1994

(9) G.V. Reklaitis, A. Ravindran, K.M. Ragsdell, Engeneering Optimalization Methods and Applications, A Wiley Interscience Publication, chap 2, chap 3.

(10) Everitt, B.S, "Cambridge Dictionary of Statstics", Cup. ISBN 0-521-81099-x, 2002

(11) Vubonite®, technical dat sheet, www.vubonite.com